Uncovering Clar's aromatic π-sextet rule in the Hubbard model using Maximum Probability Domain Partitions

Daria Tolstykh[1], Laurent Lemmens[1], Stijn De Baerdemacker[2], Dimitri Van Neck[3], Patrick Bultinck*[1], and Guillaume Acke[1]

[1]Ghent Quantum Chemistry Group, Department of Chemistry, Ghent University, Belgium
[2]Department of Chemistry, University of New Brunswick, Canada
[3]Center for Molecular Modeling, Ghent University, Belgium

December 18, 2021

Abstract

Clar's aromatic π-sextet rule is a widely used qualitative method for assessing the electronic structure of polycyclic benzenoid hydrocarbons. Unfortunately, many of the quantum chemical concordances for this rule have a limited range of applicability. Here, we show that the fundamental probabilities associated with a distribution of electrons over domain partitions support Clar's rule in both mean-field and static correlation regimes. In particular, domain partitions that maximize those probabilities reflect the dominance of Clar structures in the electronic structure of these molecules. These findings suggest that extending methods that aim to maximize probabilities by deforming domain partitions could lead to novel quantum chemical underpinnings for many chemical concepts.

Keywords: Clar's rule, Hubbard Model, Maximum Probability Domain Partitions ■

*Patrick.Bultinck@UGent.be

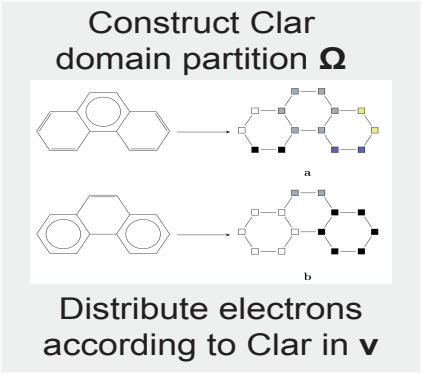

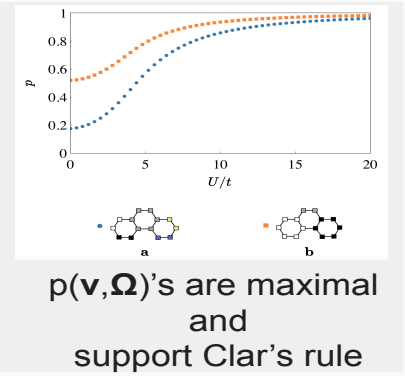

Based on the statistical interpretation of the wavefunction, MPDPs reveal optimal partitions of space into domains for which the probability to find ν *and only* ν electrons in each domain is maximal. Using this novel approach, we provide a concordance to Clar's aromatic π-sextet rule in both mean-field solutions and situations where electron correlation plays an important role.

INTRODUCTION

Armit and Robinson introduced the "aromatic sextet" as a circle inside the structure of benzene aimed at describing "groups of six electrons that resist disruption", merging[1] the concept of "six aromatic electrons" by Crocker[2] and the circle notation of Armstrong[3] (see fig. 1).

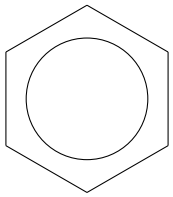

Figure 1: Armit and Robinson's representation of benzene.

Thirty years later, Clar put forward that in polycyclic benzenoid hydrocarbons (PBHs), the structures with the largest number of non-adjacent aromatic sextets best characterize their properties[4–6]. The structures that satisfy this rule are labelled as "Clar valence structures" and are constructed by drawing the highest possible number of circles (i.e. aromatic sextets) in the hexagons of the benzenoid system, provided these circles are not placed adjacent to one another. For instance, according to Clar's rule, the class of Kekulé structures that best characterizes the properties of phenanthrene is given by structure **b** in fig. 2 and one should expect the outer rings to be more benzene-like than the inner ring[7,8]. In anthracene, the application of Clar's rule leads to a "migrating sextet", i.e. a superposition of three classes of structures that are of equal importance (see fig. 3).

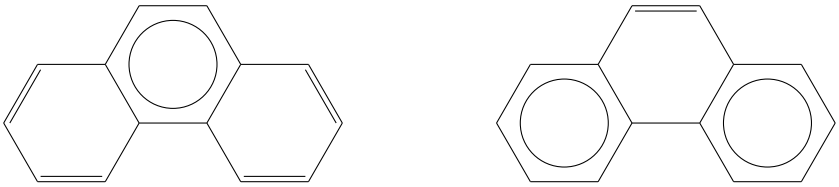

Figure 2: Phenanthrene has five Kekulé structures, divided into two classes **a** and **b**. According to Clar's rule, structure **b** is the most important, as it contains the largest number of disjoint aromatic sextets.

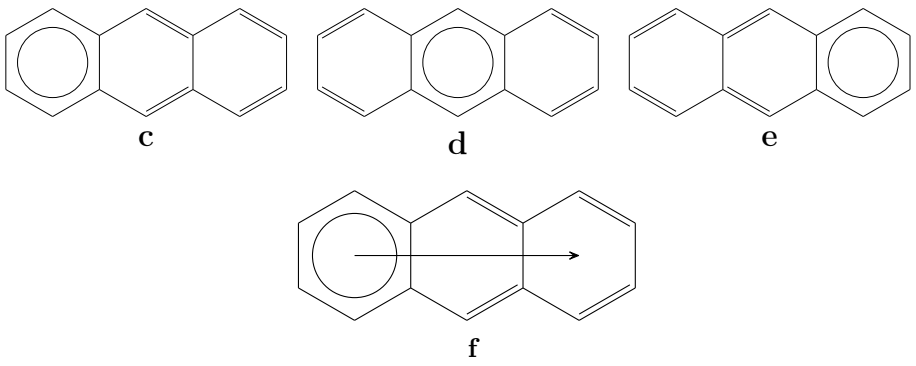

Figure 3: The Kekulé structures of anthracene can be divided into classes **c**, **d** and **e**. As Clar's rule assigns equal importance to each of these classes, the resulting Clar structure **f** is a superposition of these and is called a "migrating sextet".

These Clar structures have proven important for gaining qualitative insight in the local reactivity and other properties of PBHs[9] and have been supported by experimental findings[4,5,10–12]. Although several attempts have been made to reframe this rule quantum theoretically, finding a *unique* quantum chemical concordance has proven difficult. Among others, Polansky and Derflinger[13] measured the 'benzene character' of a ring based on the similarity of the Hückel molecular orbitals (HMOs) between those regions where the Clar structure contains an aromatic sextet and benzene itself. Later on, Bultinck et al.[14] generalized it to an ab initio level of theory based on ideas of molecular quantum similarity. Herndon and Ellzey, Randic and Aihara proposed to analyse the relative weights of valence bond (VB) resonance structures[15–18]. In turn, Aida and Hosoya[19] proposed the complementary use of HMOs and VB resonance structures in order to describe PBHs. However, as these analyses are directly based on method-specific quantities, their range of applicability is *limited* to those systems for which the level of theory used leads to sufficiently accurate descriptions. Hence, interpretations that are *not* based on those quantities are highly desirable.

The Maximum Probability Domains (MPDs) approach devised by Savin et al.[20,21] provides a unique way of *directly* assigning chemical meaning to Born's formulation[22] of the probability density function $|\Psi|^2$. Using small atomic systems, Savin showed that there is chemical utility in finding those domains Ω in spin-position space for which the probability of finding ν *and only* ν electrons inside is maximal[20]. Unfortunately, optimizing such do-

mains in spin-position space has proven difficult and has thusfar in most applications only been routinely possible for single-determinant wave functions[21] using numerically inaccurate optimization procedures[23,24], which clouds the properties of MPDs.

Recently, however, we showed[25] that in the special case of the Hubbard model[26], the theory of MPDs can be mapped to numerically accurate and efficient optimization procedures that can be applied to the exact (i.e. Full Configuration Interaction (FCI)) wave function, as well as, any approximate wave function expressed in Fock space. Furthermore, by tuning the parameters of the Hubbard model, the behavior of the MPDs in both the mean-field as well as the static correlation regime can be explored. As such, by determining the MPDs for two electrons we could show that the Kekulé and Dewar structures of benzene emerge from Hubbard model wave functions[25].

In this study, we extend the MPD framework to take the simultaneous optimization of multiple domains into account, leading to the more general theory of "Maximum Probability Domains Partitions" or MPDPs. We show that for prototypical 14-site, 14-electron ($14s, 14e^{\text{-}}$) systems (i.e. Hubbard anthracene and phenanthrene) MPDPs provide unique quantum chemical support for Clar's rule for both mean-field solutions and situations where static correlation is important.

THEORY

The theory of Maximum Probability Domain-Partitions (MPDPs) is based on four concepts: (i) domains, (ii) partitions of domains, (iii) probability measures associated with a partition of electrons over the domain partition and (iv) methods to deform the domains in order to maximize the associated probability measure. The following theory applies to the specific case of the Hubbard model site space, but can be generalized to spin-position space[27].

The Hubbard model

The Hubbard model Hamiltonian is defined in an abstract 'site' basis that depends on a semi-empirical parameter t_{ij}, that allows for intersite hopping between pairs of sites i and j,

and a site-dependent on-site energetic penalty term U_i, associated with on-site electrostatic repulsion

$$\hat{\mathcal{H}}_{\text{Hubbard}} = -\sum_{i,j=1}^{L}\sum_{\sigma=\uparrow,\downarrow} t_{ij}\hat{a}^{\dagger}_{i\sigma}\hat{a}_{j\sigma} + \sum_{i=1}^{L} U_i \hat{n}_{i\uparrow}\hat{n}_{i\downarrow}\,, \tag{1}$$

with L the number of sites and $\hat{n}_{i\sigma}$ the number operator counting the number of particles with spin σ on site i

$$\hat{n}_{i\sigma} = \hat{a}^{\dagger}_{i\sigma}\hat{a}_{i\sigma}\,. \tag{2}$$

Although the hopping matrix $\mathbf{t} = \{t_{ij}\}$ allows for hopping between any two sites, owing to the exponential decay of the on-site orbitals it usually suffices to follow the geometry of the lattice and restrict to nearest neighbor hopping. Considering phenanthrene and anthracene do not contain any heteroatoms, $\mathbf{t}$ is further simplified to

$$\mathbf{t} = t\mathbf{A} \tag{3}$$

with t a constant value and $\mathbf{A}$ the adjacency matrix reflecting the geometry of the lattice. It consists of all zeroes, except ones for all elements (i, j) if sites i and j are adjacent. In the same spirit, the on-site repulsion is regarded as site-independent. The eigenstates of the Hubbard Hamiltonian $\hat{\mathcal{H}}_{\text{Hubbard}}$ can be expanded in the orthonormal basis spanned by the eigenstates of the number operator $\hat{n}_{i\sigma}$

$$|\Psi\rangle = \sum_{[n]} c_{[n]}\,|[n]\rangle\ , \tag{4}$$

with $c_{[n]}$ the coefficient belonging to a basis state $|[n]\rangle$ labelled by the partitioning $[n] = [[n_\uparrow], [n_\downarrow]] = [[n_{1\uparrow}, \ldots, n_{L\uparrow}], [n_{1\downarrow}, \ldots, n_{L\downarrow}]]$. Depending on the problem at hand, we can represent $[n_\sigma]$ in three ways: as (i) an occupation number vector (ONV)[28] to derive theoretical expressions, (ii) a bitstring representation for computational algorithms and (iii) a graphical representation for explanatory purposes. For instance, ONV $|[1, 1, 0, 0, 0, 1], [0, 1, 0, 1, 1, 0]\rangle$ with $L = 6$ sites at half-filling, i.e. with L electrons and $\left\langle \hat{S}_z \right\rangle = 0$, can be represented graphically as

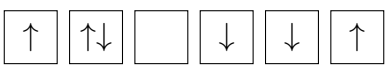

and as a bitstring as

"110001" for the ↑-component

"010110" for the ↓-component.

The values of the expansion coefficients $c_{[n]}$ are obtained by diagonalization of the Hamiltonian in eq. (1) in a Fock (sub)space and depend on the relative interaction strength U/t and the number of spin-resolved electrons N_α and N_β. At the mean-field regime $U/t \approx 0$, the Hubbard Hamiltonian leads to an idempotent density matrix and the wave function corresponds to a single Slater determinant wave function. In case of $U/t \gg 1$, static correlation breaks the idempotency of the density matrix and the wave function holds multiple quasi-degenerate states.

Domains in the Hubbard model

In the context of the Hubbard model, a domain Ω_a of size M_a is a subset of the total set of L sites. For instance, we can represent a domain Ω_a of size $M_a = 3$, consisting of the second, third and fifth site for a minimal Hubbard model of 1,3,5-hexatriene with $L = 6$ sites graphically as

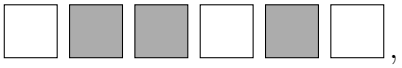

where the collection of gray blocks represents domain Ω_a. A shorthand notation $\Omega_a = \{2, 3, 5\}$, where we only specify the positions of the M_a sites within the domain, is often more convenient and employed throughout later sections. For computational purposes, we prefer a slightly different notation mimicking bitstrings

$$\Omega_a = [\omega_a] = [\omega_{a1}, \ldots, \omega_{aL}] = [0, 1, 1, 0, 1, 0]\,, \tag{5}$$

with the constraints $\forall i:\ \omega_{ai} \in \{0, 1\}$ and $\sum_{i=1}^{L} \omega_{ai} = M_a$. For each domain size M_a, there are $\binom{L}{M_a}$ domains if we do not impose any constraints on the allowed topologies of those domains.

Partitions of domains

The abstract site space can be partitioned into a collection of d non-overlapping domains

$$\mathbf{\Omega} = (\Omega_1, \ldots, \Omega_a, \ldots, \Omega_d)\,. \tag{6}$$

As such, a possible domain partition with three distinct domains Ω_1, Ω_2 and Ω_3 for 1,3,5-hexatriene can be represented graphically as

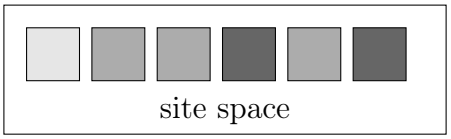

or can equivalently be written down as $(\{1\}, \{2, 3, 5\}, \{4, 6\})$.

Probability measures associated with a partition of electrons over domain partitions

The number of σ-electrons within domain Ω_a is given by overlap between the domain defined in eq. (5) and the spin-σ component of the basis state $|[n]\rangle$

$$\forall 1 \leq a \leq d:\; n_\sigma(\Omega_a) = \sum_{i=1}^{L} \delta(i \in \Omega_a) n_{i\sigma} = \sum_{i=1}^{L} \omega_{ai} n_{i\sigma}\,, \tag{7}$$

where the logical delta[29–31] $\delta(i \in \Omega_a) = 1$ if site i is an element of domain Ω_a and zero otherwise. The total number of electrons in domain Ω_a is then the sum of $\uparrow$- and $\downarrow$-electrons in that domain.

$$n(\Omega_a) = \sum_{\sigma} n_\sigma(\Omega_a) \tag{8}$$

E.g. for the given basis state above

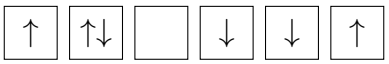

the electron partition corresponding to the domain partition introduced above is given by

where there is one $\uparrow$-electron in domain Ω_1, one $\uparrow$- and two $\downarrow$-electrons in domain Ω_2 and one $\uparrow$- and one $\downarrow$-electron in domain Ω_3.

We can determine the probability of finding ν_a *and only* ν_a electrons in each domain Ω_a by projecting out those coefficients $c_{[n]}$ of the Hubbard wavefunction in which exactly ν_a electrons occupy the sites of Ω_a. Since the number operator $\hat{n}_{i\sigma}$ is diagonal in the site basis, each basis state contributes with a factor $|c_{[n]}|^2$ to the probability[25,32].

$$P(\nu_a, \Omega_a) = \sum_{[n]} |c_{[n]}|^2 \, \delta(\nu_a = n(\Omega_a)) \tag{9}$$

For the generalization to an electron partition accompanying a d-domain partition

$$\boldsymbol{\nu} = [n(\Omega_1), \ldots, n(\Omega_a), \ldots, n(\Omega_d)] \,, \tag{10}$$

the associated probability of finding spin-independent electron partition $\boldsymbol{\nu}$ in $\boldsymbol{\Omega}$, i.e. the spin-integrated probability, is

$$P(\boldsymbol{\nu}, \boldsymbol{\Omega}) = \sum_{[n]} |c_{[n]}|^2 \left(\prod_a^d \delta(\nu_a = n(\Omega_a)) \right) . \tag{11}$$

In this paper, we will focus on spin-integrated probabilities in order to mimic Lewis' idea of the electron pair[33] as closely as possible.

Deforming domain partitions to attain maximality in the probability measure

An MPDP($\boldsymbol{\nu}$) is a domain partition for which the probability of finding a given electron partition $\boldsymbol{\nu}$ is maximized[25]

$$P(\boldsymbol{\nu}, \boldsymbol{\Omega}^*) = \max \, P(\boldsymbol{\nu}, \boldsymbol{\Omega}) \,. \tag{12}$$

As the definition of MPDPs in eq. (12) allows for local maxima, we can define the set of MPDPs for electron partition $\boldsymbol{\nu}$ in the present context as follows[25]:

$$\text{MPDPs}(\boldsymbol{\nu}) = \{ \boldsymbol{\Omega}^* | \forall \boldsymbol{\Omega} \in \epsilon_{\boldsymbol{\Omega}^*} : P(\boldsymbol{\nu}, \boldsymbol{\Omega}^*) \geq P(\boldsymbol{\nu}, \boldsymbol{\Omega}) \} \,, \tag{13}$$

where $\epsilon_{\boldsymbol{\Omega}^*}$ defines the set of domain partitions which are within a certain distance ϵ from domain partition $\boldsymbol{\Omega}^*$

$$\epsilon_{\boldsymbol{\Omega}^*} = \{ \boldsymbol{\Omega} | \| \boldsymbol{\Omega}^* - \boldsymbol{\Omega} \| \leq \epsilon \} \,. \tag{14}$$

For the Hubbard model, we can use the number of sites in which two partitions differ as a distance measure. If we set $\epsilon = 2$, this reduces to a single-site flip stability criterion, which means that the optimization allows for single sites to dissociate from one domain and merge with an other. All single-site flips for a given domain partition must preserve the number of domains to prevent loss of meaning of the electron partition associated with the probability measure. Only the domain partitions that are stable in their probability with respect to the single-site flip criterion can then be called MPDPs. For example, the above 3-domain partition $(\{1\},\{2,3,5\},\{4,6\})$ with associated probability $P(\{1\},\{2,3,5\},\{4,6\})$ can be flipped on site 2 to domain partition $(\{1,2\},\{3,5\},\{4,6\})$ with probability $P(\{1,2\},\{3,5\},\{4,6\})$.

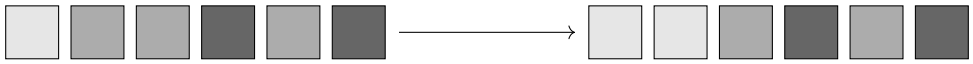

$P(\{1\},\{2,3,5\},\{4,6\})$ $\qquad$ $P(\{1,2\},\{3,5\},\{4,6\})$

Provided that $P(\{1\},\{2,3,5\},\{4,6\})$ is greater than or equal to $P(\{1,2\},\{3,5\},\{4,6\})$ and the probabilities of all other possible single-site flips, the domain partition may be called an MPDP.

METHODOLOGY

We use two systems that illustrate Clar's rule in a prototypical way: Hubbard anthracene and phenanthrene, each at half-filling $(14s, 14e^{\text{-}})$. To distinguish mean-field from static correlation regimes, we vary the interaction strength U/t of the given Hubbard model from 0 to 20 in steps of 0.1 by modifying U during the whole range while t remains constant. For each value of U/t, the corresponding Hamiltonian eigenvalue problem for each value is solved using the Davidson diagonalization method[34] in the Fock subspace of dimension $\binom{14}{7}\binom{14}{7}$ using our open-source software package `GQCP`[35]. We then define the complete set of multi-domain partitions in the site basis and each domain d in the respective partitions is then stored as a bitstring with size L. The probabilities associated with a given electron partition over all possible domain partitions are calculated using eq. (11) and tested for the single-site flip stability criterion according to eq. (14).

We note that by using 'exact solutions' (i.e. at the FCI level) our analysis is not obscured

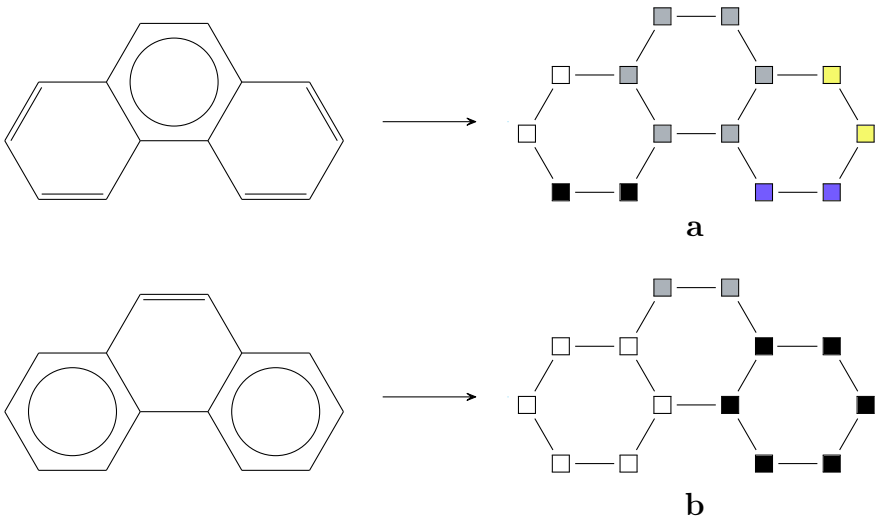

Figure 4: Pictorial representations of the domain partitions that can be associated with the structures of phenanthrene.

by possible artifacts of approximate solution methods. Unfortunately, the exponential scaling of the FCI method renders larger systems well out of reach. For example, a $16s, 16e^{-}$ system leads to a diagonalization that is approximately 200 times computationally more expensive than the Clar prototypical systems in this study.

RESULTS AND DISCUSSION

MPDPs that correspond to the highest number of disjoint sextets have higher probabilities

As is illustrated in fig. 4, we represent the classes of structures for phenanthrene as Hubbard site domain partitions. Here, the aromatic sextets are represented by domains containing 6 sites while the remaining π-electron pairs are represented by domains of size 2. As such, class **a** is represented by a 5-domain partition, consisting of a 6-ring domain and four 2-site domains. The Clar structure **b** is a 3-domain partition, with two 6-ring domains and a 2-site domain.

For a range of U/t values, we can determine the probability to find ν *and only* ν electrons in each of those domains containing ν sites (see fig. 5). The results of our shape optimization

algorithm show that all possible single-site flips reduce the associated probabilities. As such, the associated probabilities are also *maximal* and the domain partitions are MPDPs for the entire range of U/t.

In the mean-field regime (i.e. small U/t), partition **a** has a significantly lower probability than the Clar domain partition **b**. This difference in probability remains significant during the entire transition to the strongly correlated regime, where both partitions eventually converge to the same probability due to the localized anti-ferromagnetic character of the wave function. These results offer an attractive physical interpretation of Clar's sextet rule: Clar structures have a *higher probability* of occuring. As these structures have a higher probability, they influence the chemical properties of the system under study to a greater extent. At very high U/t, the large on-site repulsion forces one electron per site. As such, the probabilistic difference between both structures is strongly reduced. Figure 5 shows that Clar structures remain the most important throughout the entire U/t range and determines the range of applicability of Clar's rule. Although this rule *no longer* applies at very high U/t, it *does* apply during the *entire* transition to highly correlated regimes.

We note that our interpretation of structures in terms of domain partitions does *not* imply that "chemical bonds" are present between the sites in the domain. Indeed, *all* acceptable electron configurations (i.e. configurations that partition $\boldsymbol{\nu}$ electrons over a domain partition $\boldsymbol{\Omega}$) will contribute to the associated probability $P(\boldsymbol{\nu}, \boldsymbol{\Omega})$. The *extent* to which these configurations contribute to that probability is determined by the underlying wavefunction, which in turn captures the dynamics of the Hamiltonian. As such, even electron configurations where the electrons in a given domain do not interact *directly* according to the underlying Hamiltonian can contribute to the associated probability.

MPDPs that correspond to migrating sextets have similar probabilities

We can represent the classes of structures for anthracene as Hubbard site domains as illustrated in fig. 6. As such, each structure translates to a 5-domain partition, consisting of a 6-ring domain and four 2-site domains. The probability to find ν *and only* ν electrons in each

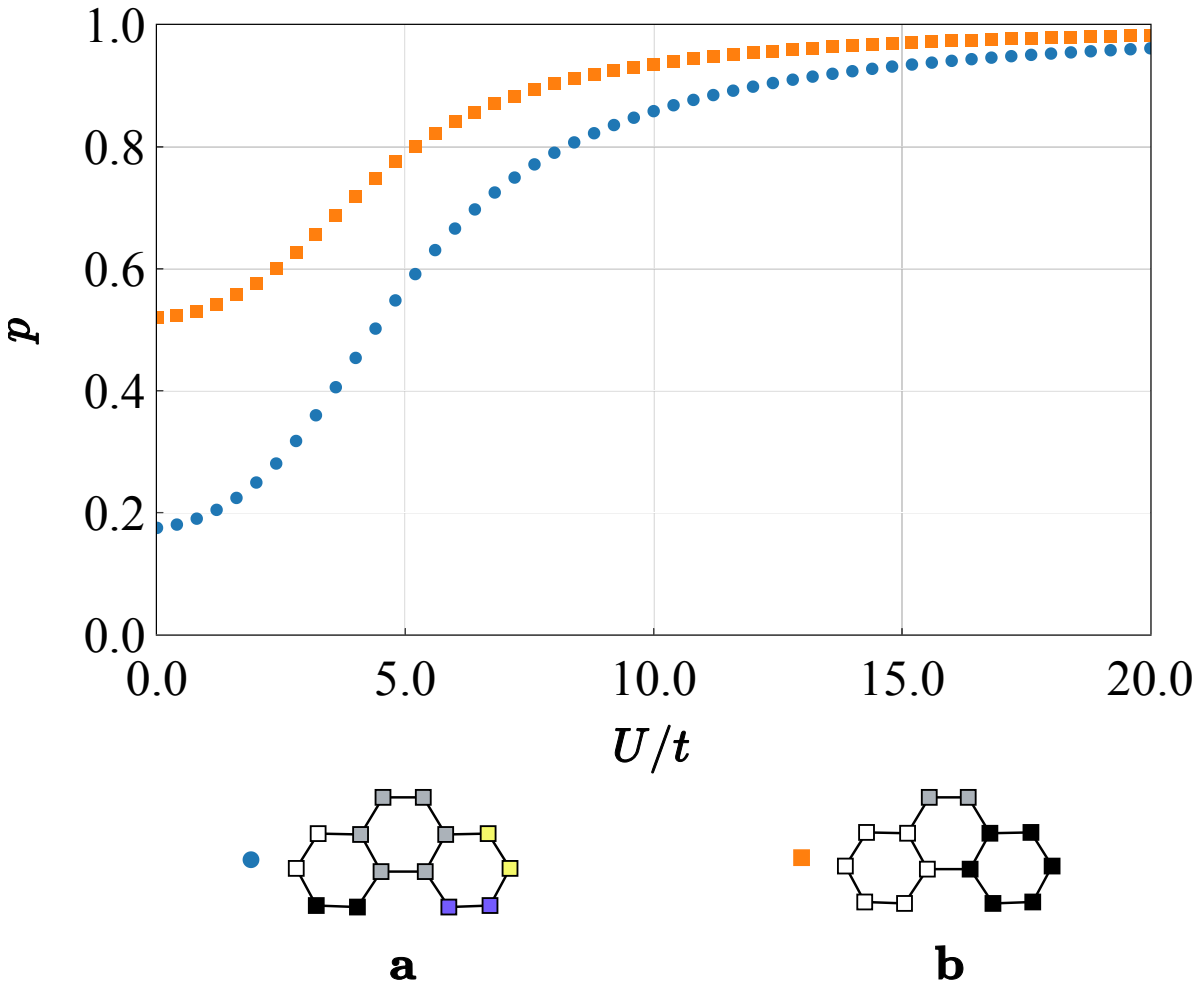

Figure 5: MPDPs in terms of aromatic sextets for a 2D Hubbard of phenanthrene at half-filling for different U/t values.

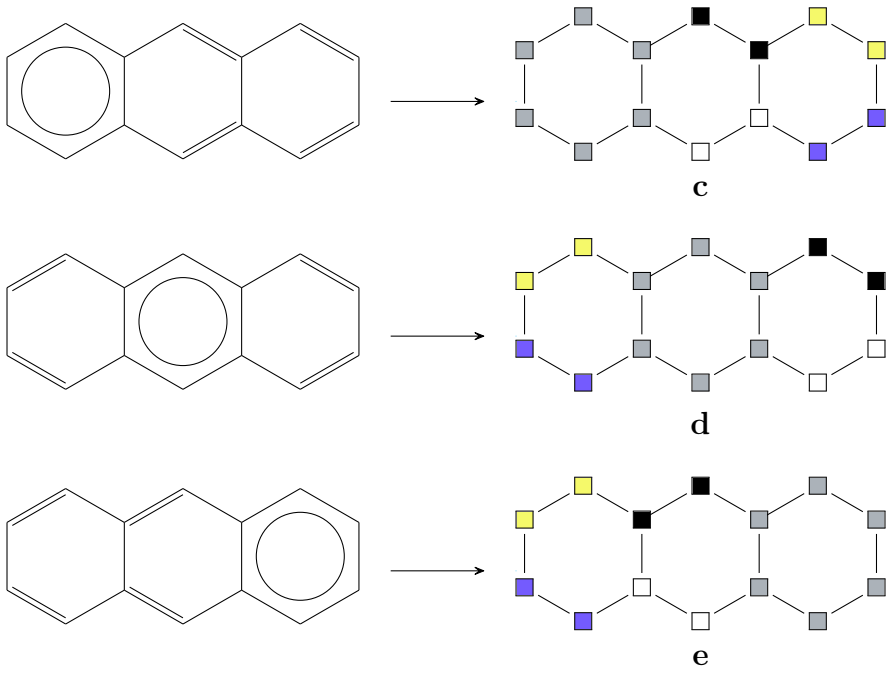

Figure 6: Pictorial representations of the domain partitions that can be associated with the structures of anthracene.

of those domains containing ν sites is maximized for a range of U/t values (see fig. 7). Again, most importantly, all partitions are MPDPs for the entire range of U/t as their probabilities remain maximal for each U/t. In the mean-field regime, partition **d** only has a (slightly) higher probability than the other partitions **c** and **e**. This slight difference becomes even smaller with rising U/t and becomes negligible at very high U/t. These results offer a physical interpretation of Clar's migrating sextet: as all partitions have the *same probability* of occuring they influence the chemical properties of the system to an *equal* extent. Again, this rule applies to the entire U/t range, although it is trivially satisfied at very high U/t as one electron is forced on each site.

Intriguingly, Clar was forced to propose an additional non-Kekulé structure[6] for anthracene with two aromatic sextets and the localization of two electrons at the 1,4-region of the inner ring (fig. 8) to account for the chemical reactivity at its 9,10-positions. Following Clar's idea as closely as possible, we construct the corresponding 3-domain partition **f** by two 6-ring domains and a 2-site domain at the para positions of the inner ring. A similar analysis as above shows that the corresponding MPDP in fig. 9 has a higher prob-

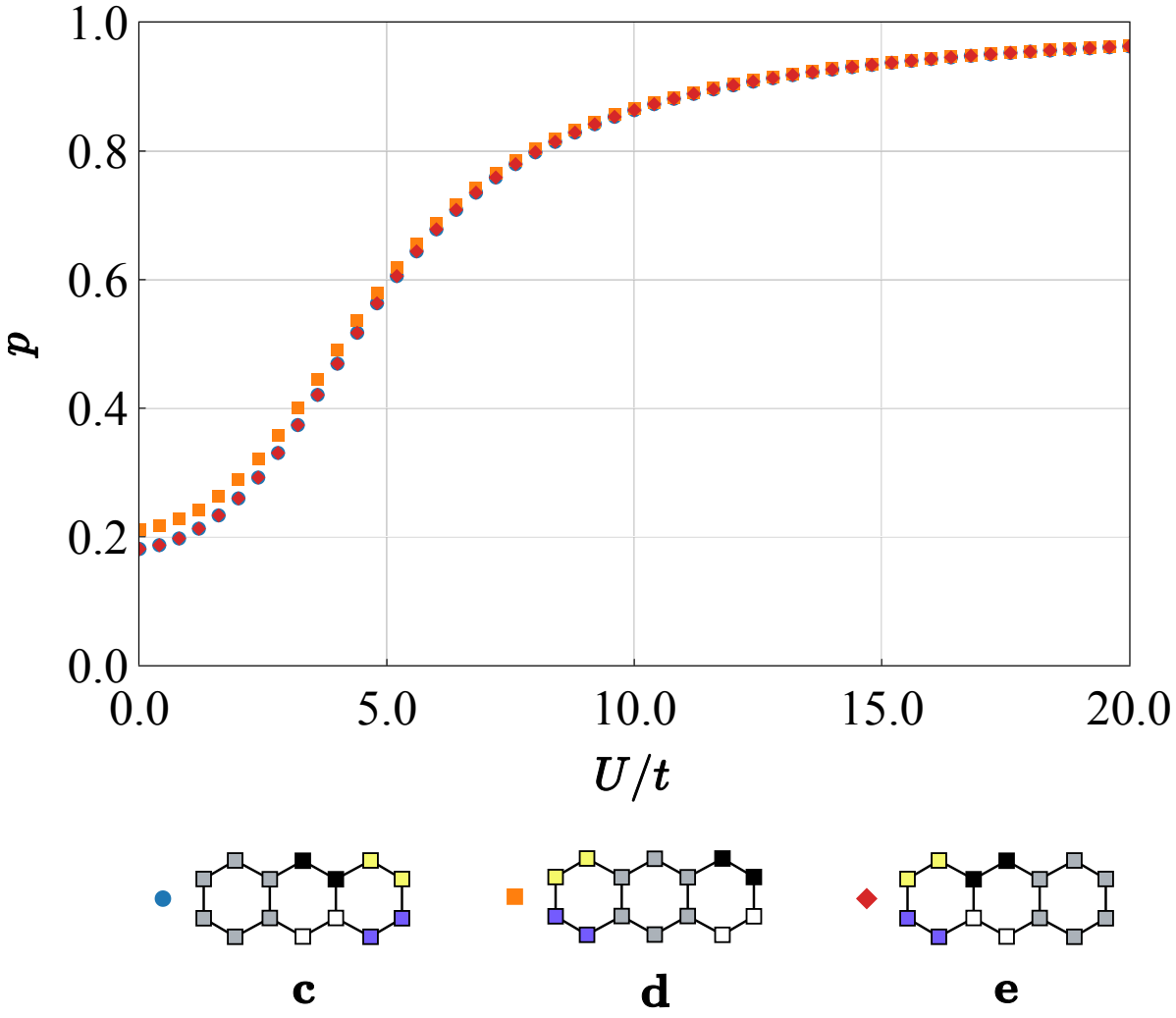

Figure 7: MPDPs portraying the migrating aromatic sextet for a 2D Hubbard of anthracene at half-filling for different U/t values.

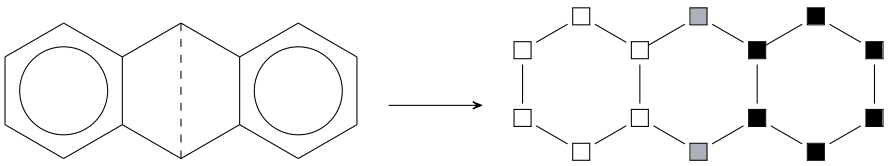

f

Figure 8: Clar structure for anthracene with two aromatic sextets separated by a localization of two electrons at the 1,4-region of the inner ring, along with its pictorial representation of the domain partition.

ability than each of the MPDPs associated with the migrating sextet. As such, this result provides probabilistic support for Clar's proposal to augment the description of anthracene with a non-Kekulé structure: this structure has a high probability of occuring and therefore influences the reactivity of this system.

We note that the theoretical reasons *why* MPDPs exhibit the above concordances lie hidden within the vast amount of information in the FCI wavefunction. On the other hand, Clar based his rule on Lewis structures, which are defined within Lewis theory. As such, MPDPs offer a "road that connects two sciences (quantum chemistry and Lewis theory) that are not visible from the viewpoint of one science alone"[36].

CONCLUSIONS

In this study, we show that MPDP analyses of two prototypical systems lead to chemically meaningful domains that concord with Clar structures and that the associated probabilities quantitatively favor the same structures as Clar's rule. As MPDPs do not directly depend on method-specific quantities that often have a limited range of applicability, we could show that in the Hubbard model Clar's rule remains valid both in the mean-field and in the statically correlated regime.

These results indicate that methods where domains are deformed to maximize probabilities have great potential to deliver novel interpretational tools for extracting important chemical concepts from quantum chemical wave functions. As such, porting these techniques from the realm of model Hamiltonians to quantum chemical spin-position space is

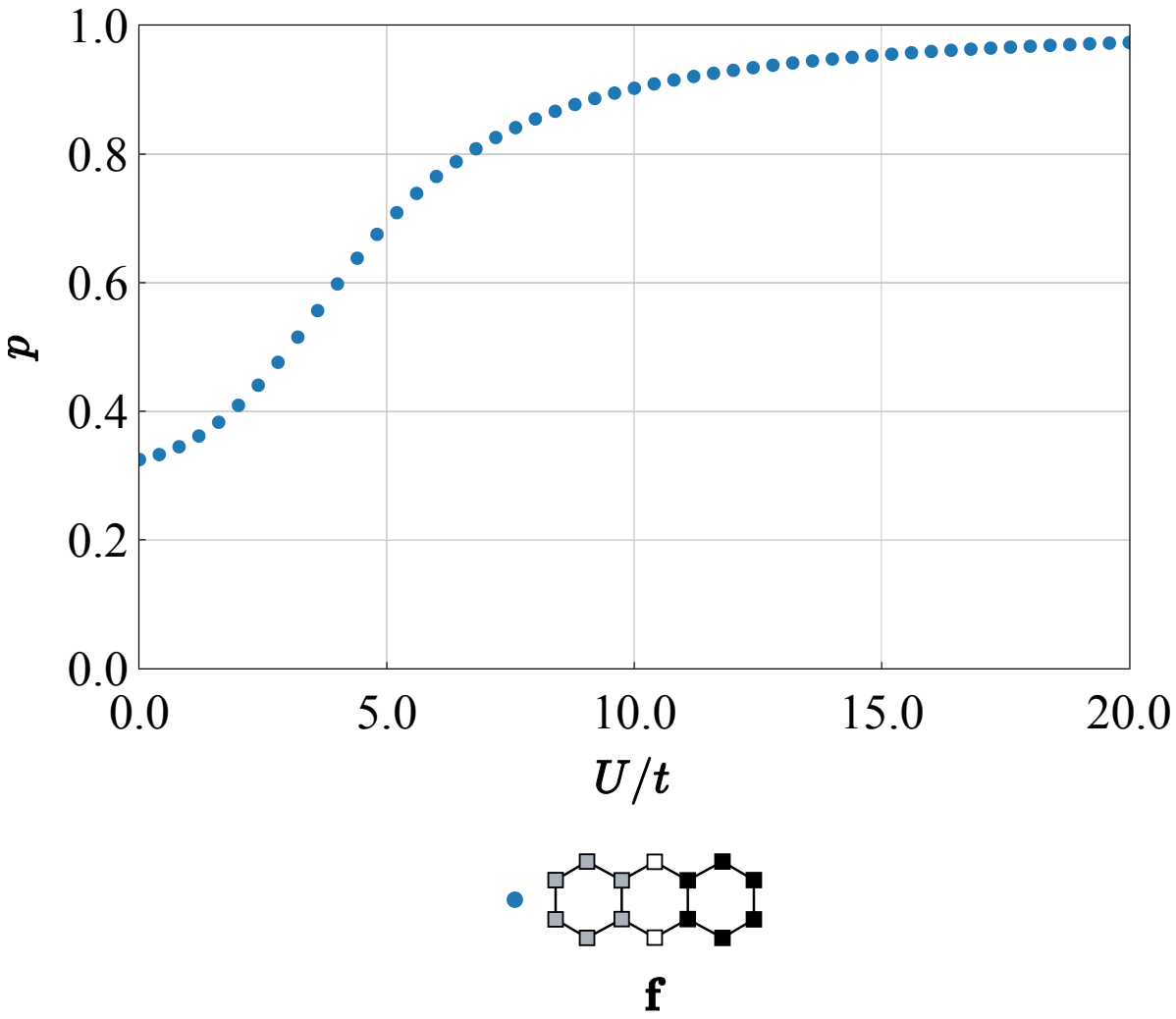

Figure 9: MPDP characterizing two aromatic sextets separated by a localization of two electrons at the 1,4-region of the inner ring for a 2D Hubbard of anthracene at half-filling for different U/t values.

particularly worth exploring further.

ACKNOWLEDGMENTS

This research was funded by the Special Research Fund of Ghent University (Research Project BOF/24J/2019/061). The computational resources (Stevin Supercomputer Infrastructure) and services used in this work were provided by the VSC (Flemish Supercomputer Center), funded by Ghent University, FWO, and the Flemish Government-Department EWI. L.L. acknowledges support from an FWO Ph.D. fellowship (Grant No. 1126619N). SDB acknowledges financial support from the NSERC Canada Research Chair program.

DATA AVAILABILITY STATEMENT

The code and data that support the findings of this study are available from the corresponding author upon request.

References

1. A. T. Balaban, P. v. R. Schleyer, and H. S. Rzepa, Chem. Rev. **105**, 3436 (2005), URL https://doi.org/10.1021%2Fcr0300946.

2. E. C. Crocker, J. Am. Chem. Soc. **44**, 1618 (1922), URL https://doi.org/10.1021/ja01429a002.

3. H. E. Armstrong, Proc. Chem. Soc. **6**, 101 (1890), URL https://doi.org/10.1039/PL8900600095.

4. E. Clar and M. Zander, J. Chem. Soc. p. 1861 (1958), URL https://doi.org/10.1039%2Fjr9580001861.

5. E. Clar, *Polycyclic Hydrocarbons - Volume I* (Springer-Verlag Berlin Heidelberg GmbH, 1964).

6. E. Clar, *The Aromatic Sextet* (John Wiley & Sons, Ltd., 1972).

7. J. M. Schulman and R. L. Disch, J. Phys. Chem. A **103**, 6669 (1999), URL https://doi.org/10.1021/jp9910587.

8. M. K. Cyrański, B. T. Sępień, and T. M. Krygowski, Tetrahedron **56**, 9663 (2000), ISSN 0040-4020, URL https://doi.org/10.1016/S0040-4020(00)00919-4.

9. M. Solà, Front. Chem. **1**, 1 (2013), URL https://doi.org/10.3389%2Ffchem.2013.00022.

10. E. Clar and W. Schmidt, Tetrahedron **35**, 2673 (1979), ISSN 0040-4020, URL https://doi.org/10.1016/0040-4020(79)87049-0.

11. D. Biermann and W. Schmidt, Journal of the American Chemical Society **102**, 3163 (1980), URL https://doi.org/10.1021%2Fja00529a046.

12. D. Biermann and W. Schmidt, Isr. J. Chem. **20**, 312 (1980), URL https://doi.org/10.1002/ijch.198000090.

13. O. E. Polansky and G. Derflinger, Int. J. Quantum Chem. **1**, 379 (1967), URL https://doi.org/10.1002/qua.560010412.

14. P. Bultinck, R. Ponec, A. Gallegos, S. Fias, S. Van Damme, and R. Carbó-Dorca, Croatica Chemica Acta **79**, 363 (2006), URL https://hrcak.srce.hr/5628.

15. H. Hosoya and K. Hosoi, J. Chem. Phys. **64**, 1065 (1976), URL https://doi.org/10.1063/1.432316.

16. W. C. Herndon and M. L. Ellzey, J. Am. Chem. Soc. **96**, 6631 (1974), URL https://doi.org/10.1021%2Fja00828a015.

17. M. Randić, Tetrahedron **31**, 1477 (1975), URL https://doi.org/10.1016/0040-4020(75)87084-0.

18. J. Aihara, Bull. Chem. Soc. Jpn. **49**, 1429 (1976), URL https://doi.org/10.1246%2Fbcsj.49.1429.

19. M. Aida and H. Hosoya, Tetrahedron **36**, 1317 (1980), ISSN 0040-4020, URL https://www.sciencedirect.com/science/article/pii/0040402080850435.

20. A. Savin, in *Reviews of Modern Quantum Chemistry* (WORLD SCIENTIFIC, 2002), pp. 43–62, URL https://doi.org/10.1142%2F9789812775702_0003.

21. E. Cancès, R. Keriven, F. Lodier, and A. Savin, Theor. Chem. Acc. **111**, 373 (2004), URL https://doi.org/10.1007%2Fs00214-003-0509-4.

22. M. Born, Zeitschrift für Physik **37**, 863 (1926), URL https://doi.org/10.1007%2Fbf01397477.

23. O. M. Lopes, B. Braïda, M. Causà, and A. Savin, *Advances in the Theory of Quantum Systems in Chemistry and Physics - Understanding Maximum Probability Domains with Simple Models* (Springer, 2012).

24. M. Menéndez and A. M. Pendás, Theor. Chem. Acc. **113**, 1 (2014), URL https://doi.org/10.1007/s00214-014-1539-9.

25. G. Acke, S. De Baerdemacker, P. Claeys, M. Van Raemdonck, W. Poelmans, D. Van Neck, and P. Bultinck, Mol. Phys. (2016), URL https://doi.org/10.1080/00268976.2016.1153742.

26. J. Hubbard, Proc. R. Soc. A **276**, 238 (1963), URL https://doi.org/10.1098%2Frspa.1963.0204.

27. G. Acke, S. De Baerdemacker, Á. M. Pendás, and P. Bultinck, Wiley Interdiscip. Rev. Comput. Mol. Sci. **10**, 1 (2019), URL https://doi.org/10.1002/wcms.1456.

28. T. Helgaker, P. Jørgensen, and J. Olsen, *Molecular Electronic-Structure Theory* (John Wiley & Sons, Ltd. - Chichester, 2000).

29. R. Carbó-Dorca and E. Besalú, J. Math. Chem. **13**, 331 (1993), URL https://doi.org/10.1007%2Fbf01165573.

30. R. Carbó and E. Besalú, Comput. Chem. **18**, 117 (1994), ISSN 0097-8485, URL https://www.sciencedirect.com/science/article/pii/0097848594850054.

31. R. Carbó-Dorca and E. Besalú, J. Math. Chem. **18**, 37 (1995), URL https://doi.org/10.1007/BF01166602.

32. E. Francisco, A. M. Pendás, and M. A. Blanco, J. Chem. Phys. **126**, 094102 (2007), URL https://doi.org/10.1063%2F1.2709883.

33. G. N. Lewis, J. Am. Chem. Soc. **38**, 762 (1916), URL https://doi.org/10.1021/ja02261a002.

34. E. R. Davidson, J. Comput. Phys. **17**, 87 (1975), ISSN 0021-9991, URL https://doi.org/10.1016/0021-9991(75)90065-0.

35. L. Lemmens, X. De Vriendt, D. Tolstykh, T. Huysentruyt, P. Bultinck, and G. Acke, J. Chem. Phys. **155**, 084802 (2021), URL https://doi.org/10.1063%2F5.0057515.

36. P. W. Anderson, Science **177**, 393 (1972), URL https://www.jstor.org/stable/1734697.